Agricultural and Forest Meteorology 250–251 (2018) 376–387

Contents lists available at ScienceDirect

Agricultural and Forest Meteorology

journal homepage: www.elsevier.com/locate/agrformet

Research paper

Strong radiative effect induced by clouds and smoke on forest net ecosystem productivity in central Siberia

Sung-Bin Park[a,*], Alexander Knohl[b,c], Antje M. Lucas-Moffat[d,1], Mirco Migliavacca[a], Christoph Gerbig[a], Timo Vesala[e,f], Olli Peltola[e], Ivan Mammarella[e], Olaf Kolle[a], Jošt Valentin Lavrič[a], Anatoly Prokushkin[g], Martin Heimann[a,e]

[a] Max Planck Institute for Biogeochemistry, Hans-Knöll-Str. 10, 07745 Jena, Germany
[b] University of Göttingen, Bioclimatology, Faculty of Forest Science and Forest Ecology, Büsgenweg 2, 37077, Göttingen, Germany
[c] University of Göttingen, Centre of Biodiversity and Sustainable Land Use (CBL), Grisebachstraße 6, 37073, Göttingen, Germany
[d] Thünen Institute of Climate-Smart Agriculture, Bundesallee 50, 38116, Braunschweig, Germany
[e] Division of Atmospheric Sciences, Department of Physics, University of Helsinki, P.O. Box 68, 00014 Helsinki, Finland
[f] Department of Forest Sciences, P.O. Box 27, FI-00014, University of Helsinki, Helsinki, Finland
[g] V. N. Sukachev Institute of Forest, Siberian Branch, Russian Academy of Sciences, Akademgorodok 50/28, Krasnoyarsk 660036, Russia

ARTICLE INFO

Keywords:
Eddy covariance
Net ecosystem productivity
Smoke
Photosynthetically active radiation
Artificial neural networks
Central Siberia

ABSTRACT

Aerosols produced by wildfires are a common phenomenon in boreal regions. For the Siberian taiga, it is still an open question if the effects of aerosols on atmospheric conditions increase net CO_2 uptake or photosynthesis. We investigated the factors controlling forest net ecosystem productivity (NEP) and explored how clouds and smoke modulate radiation as a major factor controlling NEP during fire events in the years 2012 and 2013. To characterize the underlying mechanisms of the NEP response to environmental drivers, Artificial Neural Networks (ANNs) were trained by eddy covariance flux measurements nearby the Zotino Tall Tower Observatory (ZOTTO). Total photosynthetically active radiation, vapour pressure deficit, and diffuse fraction explain at about 54–58% of NEP variability. NEP shows a strong negative sensitivity to VPD, and a small positive to f_{dif}. A strong diffuse radiation fertilization effect does not exist at ZOTTO forest due to the combined effects of low light intensity, sparse canopy and low leaf area index. Results suggests that light intensity and canopy structure are important factors of the overall diffuse radiation fertilization effect.

1. Introduction

The high northern latitudes (> 55°N) are one of the largest carbon sink regions and have become warmer and drier due in recent decades to rising temperatures (Forkel et al., 2016). Moreover, boreal forests in Russia, so-called "taiga", comprise about 21% of the world's forest area (Tishkov, 2002). Despite its importance to the terrestrial carbon cycle, this area is one of the most data-deficient regions because of its remoteness. One of the critical disturbance factors in the taiga are large wildfires induced by a combination of human activity and climate change (Achard et al., 2008; Vasileva et al., 2011; Tautenhahn et al., 2016; Tchebakova et al., 2009; Furyaev et al., 2001). Since 1996 a significant increase in the number and frequency of wildfires, as well as burned areas, has been observed (Ponomarev et al., 2016; Antamoshkina and Korets, 2015). For instance, heavy smoke from wildfires covered central Siberia in the summers of 2012 and 2013 (Ponomarev, 2013). This heavy smoke resulted in reduced incoming solar radiation and caused changes in the surface radiation balance (Schafer et al., 2002a,b).

Solar radiation, in particular photosynthetically active radiation (PAR: 400–700 nm), controls canopy processes related to photosynthesis such as gross primary productivity (GPP), net ecosystem exchange of CO_2 (NEE), and light use efficiency (LUE). Determining the biophysical and physiological mechanisms influencing canopy photosynthesis under cloudy and smoky conditions has been difficult due to the interaction among multiple environmental factors such as incoming radiation, diffuse radiation or diffuse fraction, leaf temperature, air humidity, and/or surface wetness (Dengel and Grace, 2010; Doughty et al., 2010; Gu et al., 2002, 1999; Hollinger et al., 1994; Knohl and Baldocchi, 2008; Misson et al., 2005; Rocha et al., 2004). Under cloudy, overcast or high fire-related aerosol load conditions, the total radiation reaching the canopy is reduced, typically resulting in a reduction in

* Corresponding author.
E-mail address: spark@bgc-jena.mpg.de (S.-B. Park).
[1] Now also at German Meteorological Service, Centre for Agrometeorological Research, Bundesallee 50, 38816 Braunschweig, Germany.

http://dx.doi.org/10.1016/j.agrformet.2017.09.009
Received 19 April 2017; Accepted 19 September 2017
Available online 10 January 2018

photosynthesis (Cirino et al., 2014; Yamasoe et al., 2006).

The diffuse radiation fertilization (DRF) effect is an increase in photosynthesis that results from a trade-off between decreased solar radiation and increased light scattering, both caused by clouds or smoke (Mercado et al., 2009; Rap et al., 2015; Roderick et al., 2001). Diffuse radiation enhances photosynthesis because diffuse light can more effectively penetrate the canopy (Dengel et al., 2015; Doughty et al., 2010; Knohl and Baldocchi, 2008; Urban et al., 2007; Yamasoe et al., 2006). This effect, however, depends on properties of vegetation structure properties, such as canopy architecture, leaf area index (LAI), and plant functional type (PFT) (Alton et al., 2007; Kanniah et al., 2012; Knohl and Baldocchi, 2008; Niyogi et al., 2004). Under diffuse light conditions, the efficiency of canopy photosynthesis increased substantially for both crops and forests (Choudhury, 2001; Gu et al., 2002; Niyogi et al., 2004), but not in wetlands due to their low canopy height and low LAI (Letts et al., 2005). Synthetic and data-based modelling studies have also shown that results differ significantly for the same PFT, which may be explained by differing model assumptions, treatment of radiation, and the complexity level of each model (Alton, 2008; Alton et al., 2007; Knohl and Baldocchi, 2008; Matsui et al., 2008; Mercado et al., 2009; Rap et al., 2015; Still et al., 2009). Therefore, it is still an open question how forest ecosystems respond to various light regimes (Cheng et al., 2015; Dengel and Grace, 2010; Kanniah et al., 2012; Misson et al., 2005; Oliphant et al., 2011; Strada et al., 2015).

Aerosol particles have a significant influence on photosynthesis by increasing diffuse radiation, exhibiting favorable conditions for photosynthesis similar to those created by cloudy conditions (Gu et al., 2003; Niyogi et al., 2004; Rap et al., 2015). The aerosol scattering effect may increase the amount of diffuse light, enhancing the CO_2 uptake of forests at midday by up to 8%, without reducing incoming solar radiation (Misson et al., 2005). This effect is more pronounced in forests and croplands than in grasslands (Jing et al., 2010; Niyogi et al., 2004). Another study in grassland did not find significant increases of CO_2 uptake due to aerosol loading (Kanniah et al., 2010). In tropical forests, an increase of aerosol optical depth (AOD) results in an increase of CO_2 uptake, particularly in the sub-canopy (Doughty et al., 2010; Yamasoe et al., 2006). However, if AOD is very high (> 2) or cloud cover is thick, CO_2 uptake decreases due to the reduction of incoming radiation (Cirino et al., 2014; Oliveira et al., 2007; Yamasoe et al., 2006). This suggests that moderate aerosol concentrations increase CO_2 uptake at ecosystem scales because of the DRF effect, whereas high levels of aerosols reduce CO_2 uptake by blocking solar radiation (Kanniah et al., 2012; Strada and Unger, 2016).

In this study, we use flux measurements obtained by the eddy covariance (EC) technique at the ZOtino Tall Tower Observatory (ZOTTO) site in central Siberia (Heimann et al., 2014; Kozlova et al., 2008; Winderlich et al., 2010) to understand the underlying processes of the DRF effect in a boreal forest during wildfire events. To our knowledge, no other study has investigated the effect of smoke and clouds on NEP at an ecosystem scale in central Siberia.

The objectives of this study are: (1) to characterize the environmental controls of Net Ecosystem Productivity (NEP) and (2) to examine the impact of clouds and smoke on radiation partitioning and its influence on NEP. To address these objectives we first identified the environmental drivers of NEP using an Artificial Neural Networks (ANNs) model (Moffat et al., 2010). We then tested the hypothesis that different levels of smoke particles influence NEP, enhancing it at intermediate levels and decreasing it at higher smoke levels.

2. Materials and methods

2.1. Study site

The research area is situated on the western side of the Yenisei river basin in the middle taiga subzone (Heimann et al., 2014; Kozlova et al., 2008; Winderlich et al., 2010; Fig. 1 bottom). Long-term energy and mass exchange measurements based on the EC technique in this region were performed quasi-continuously from 1998 to 2000 and 2002 to 2005 (Arneth et al., 2006; Kelliher et al., 1999; Lloyd et al., 2002; Schulze et al., 2002; Tchebakova et al., 2015). A new flux tower (60°48′25″N, 89°21′27″E, 180 m a.s.l.) was erected at a distance of 900 m from the tall tower site in mid-June 2012 (Winderlich et al., 2014; Fig. 1 top). This station is located in a homogeneous Scots pine (*Pinus sylvestrisis* L.) forest, with an average canopy height of 20 m, similar to the former site. However, the average tree age is estimated to be more than 100 years younger compared to the old site (82–107 and 230 years, respectively). The forest around Zotino is an open stand with sparse understory and a lichen-dominated ground cover (Wirth et al., 1999). The estimated stand density is 448 ± 88 trees ha^{-1} (mean ± standard deviation). The LAI value was not available during the measurement period, however, it may be the value in the range reported at the old station (1.3 $m^2 m^{-2}$ for minimum and 3.5 $m^2 m^{-2}$ for maximum) due to the sparse canopy structure (Alton et al., 2005; Los et al., 2000; Shibistova et al., 2002; Wirth et al., 1999). The forest is located on alluvial sandy mineral soil with no underlying permafrost (Kelliher et al., 1999; Lloyd et al., 2002).

2.2. Measurement systems

2.2.1. Eddy covariance flux measurements

The EC system consists of a three-axis ultrasonic anemometer USA-1 (METEK GmbH, Elmshorn, Germany) to measure three wind components as well as sonic temperature, and a closed-path infrared gas analyzer LI-7200 (LI-COR Biosciences, Lincoln, NE, USA) to measure CO_2 and H_2O concentrations. The sampling intake line consists of a 1 m stainless steel tube with an inner diameter of 7.7 mm (a 3/8″ tube). The flow rate inside the sampling line was 15 L min^{-1}, which should provide turbulent airflow inside the tubing to minimize frequency losses. The horizontal and vertical sensor separations were 25 cm and 5 cm, respectively. The voltage signals for CO_2 and H_2O concentrations (dry mole fractions) of the gas analyzer were connected to the analog input channels of the sonic anemometer. After the analog-to-digital conversion by the converter inside the anemometer, these signals were added to the digital data stream sent from the sonic anemometer to the computer via serial data transmission at a sampling rate of 20 Hz. Storage of the raw data was managed by the program EddyMeas as part of the EddySoft package (Kolle and Rebmann, 2007). Additionally the LI-7200 was directly connected to the computer via RS-232 and the program LI7200Log collected all status information and measured data from the gas analyzer at a rate of 1 Hz and stored them as 30 min averages.

In order to determine the CO_2 storage flux below the EC measurement height, ambient CO_2 concentrations were measured at nine heights (0.1, 0.3, 1, 2, 5, 9, 15, 22, 29.2 m) with a GMP343 probe (Vaisala, Helsinki, Finland). A CR10X data logger (Campbell Scientific, Logan, UT, USA) was used to control the gas-switching unit and to collect the data from the probe. Air was drawn through equal length tubes at a rate of 7 L min^{-1}, with each height being sampled for 1 min (the lowest level was sampled for 2 min). Readings were taken at a rate of 1 Hz over the last 50 s (110 s for lowest level) of sampling at each height and then averaged for each 10 min cycle before being stored. Storage fluxes of CO_2 below the flux measurement level were determined as the time change of an integrated spline function through the CO_2 profile measurements. Manual calibration of the LI-7200 and replacement of new filters were performed periodically (April, June, and September) in each measurement year.

2.2.2. Auxiliary measurements

Along with the flux measurements, meteorological data were collected. Air temperature (T_a) and relative humidity (RH) were measured

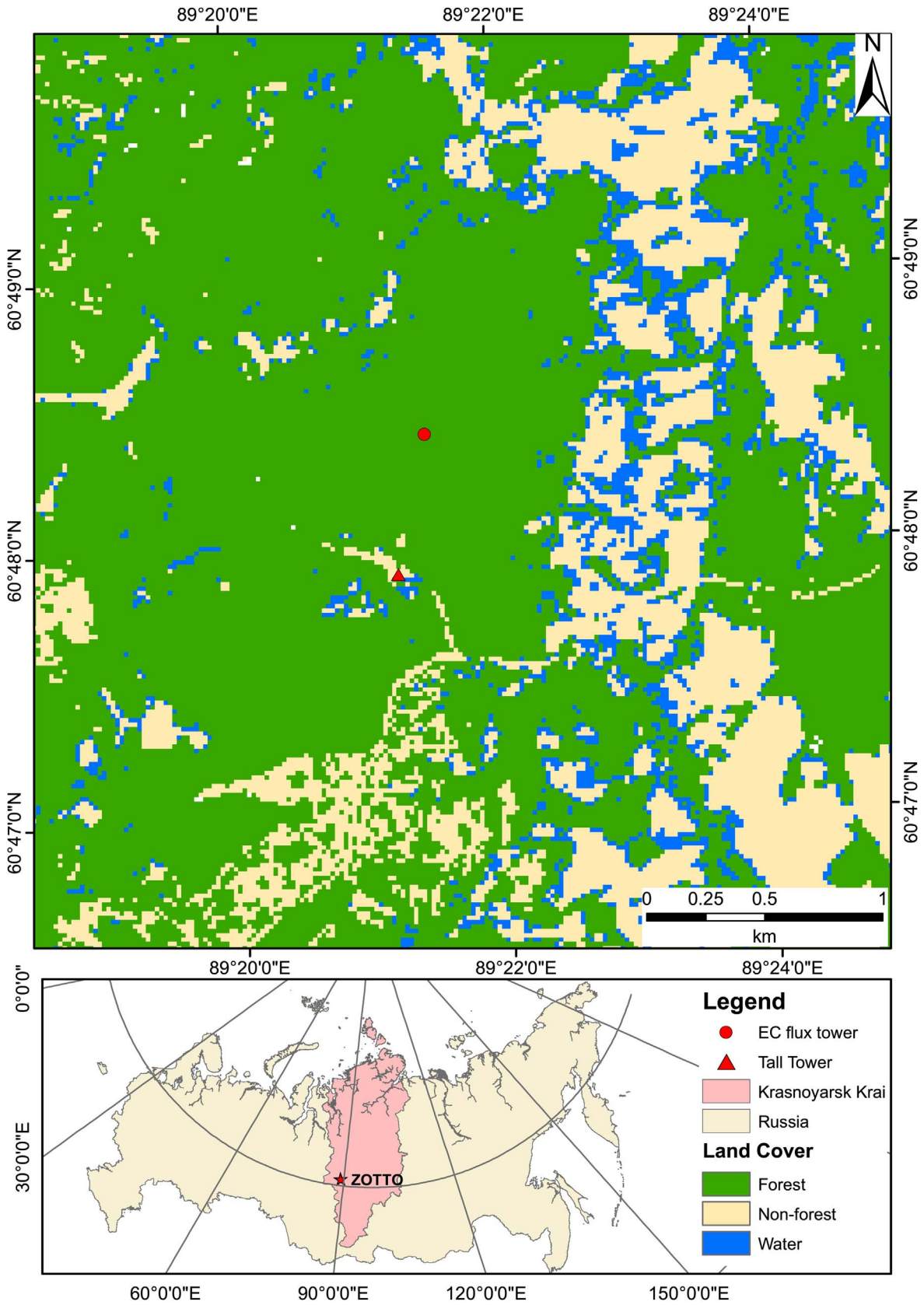

Fig. 1. Land cover (top) and geographical location (bottom) of the ZOTTO site. Land cover map is derived from 30-m Landsat-8 imagery. Round circle and triangle shapes indicate the forest eddy covariance flux tower and the tall tower sites.

at a height of 29.7 m a.g.l. with a KPK1/6-ME-H38 sensor (MELA Sensortechnik GmbH, Galltec, Germany). Atmospheric pressure was measured with a barometric pressure sensor (61302 V – RM Young Co., Traverse City, MI, USA) both above the canopy and inside of the measurement cabin. The atmospheric vapor pressure deficit (VPD) was calculated as the difference between the saturation and actual vapor pressure. Average wind velocity and wind direction were recorded using the sonic anemometer of the EC system mounted at the top of the tower. The short- and longwave radiation components were measured with a CNR1 net radiometer (Kipp & Zonen, Delft, The Netherlands) above the canopy. Up- and downward PAR were measured using a quantum sensor PQS1 (Kipp & Zonen, Delft, Netherlands). Diffuse and total PAR at 2 m height was measured using a BF-3 (Delta-T Devices Ltd., Cambridge, UK) at the tall tower station (Fig. 1 top) since 2009 (Winderlich et al., 2010).

Soil temperature was measured with PT100 probes (Jumo GmbH, Germany) at six depths (0.02, 0.04, 0.08, 0.16, 0.32, and 0.64 m). Soil moisture probes (ML-2x, DeltaT Devices, Cambridge, UK) were installed at depths of 0.08 (two replicates), 0.16, 0.32, and 0.64 m. Ground heat fluxes were measured using five heat flux plates, (HF3/CN3, McVan Instruments, Australia) installed at a depth of 0.03 m. Precipitation was collected by a heated tipping-bucket rain gauge (5.4032.35.009, Adolf Thies GmbH, Germany) at a height of 1.5 m above the ground. All ancillary measurements were collected every 10 s and then averaged every 10 min using a CR3000 data logger (Campbell Scientific, Logan, UT, USA).

For the daily AOD at 550 nm, we used the MODIS Level 2 (MOD08_D3.051) data containing the ZOTTO site from 2007 to 2013, which has a spatial resolution of 1° by 1° (http://giovanni.gsfc.nasa.gov/).

2.3. Data processing and quality control

EC data were post-processed with the EddyUH software (Mammarella et al., 2016). Data processing and flux calculations were performed in a similar manner to Mammarella et al. (2015). The high frequency CO_2 and H_2O concentration data were de-spiked by comparing two adjacent data points: if their differences were larger than 5 ppm and 10 mmol mol^{-1}, the following point was replaced with the same value as in the previous point. A double rotation method was performed during the half-hourly averaging period. A cross-wind correction was applied point by point to the sonic temperature data (Liu et al., 2001). A primary value for the time lag between the vertical wind velocity and scalar measurements was estimated for each 30 min averaging period by maximizing the covariance. The obtained values were later fine-tuned using the time lag optimizer (Mammarella et al., 2016). Fluxes were corrected for high- and low- frequency losses due to the limited frequency responses of the EC system. The response times used in correcting fluxes for low-pass filtering with a transfer function are described by Horst (1997). The transfer function of the high-pass filtering was performed as described in Rannik and Vesala (1999). The transfer function for H_2O was calculated from different classes of relative humidity (Mammarella et al., 2009).

The flux data were screened to remove erroneous values, which did not fulfil the theoretical requirements of the EC method. Half-hourly flux data were flagged as low quality if the absolute values of the skewness of the related concentration or vertical wind velocity were outside of the range (−2, 2), or if the kurtosis was outside of the range (1, 8) (Vickers and Mahrt, 1997). Furthermore, the non-steady state and the integral turbulent characteristics tests were applied following Foken and Wichura (1996). To avoid erroneous data due to malfunction of the gas analyzer, mole fractions of CO_2 and H_2O were taken in the range of [370, 450 ppmv] and [0,30 mmol mol^{-1}], respectively. In addition to these criteria, the LI-7200 data were screened based on the diagnostic values provided by the instrument. Periods were excluded if 1) the half-hourly mean values for the diagnosis of the chopper and the detector of the gas analyzer were not zero, 2) the signal strength was detected for less than 50% of the time, 3) the signal strength deteriorated with time, or 4) the signal strength was unstable. A threshold of 0.2 m s^{-1} for friction velocity (u_*) was determined based on the summer period of the first year using the algorithm described in Papale et al. (2006) and implemented in REddyProc package in R (ver. 3.2.3: R Core Team, 2016), then applied to the entire dataset. In this study we did not apply gap-filling and only used good quality measured data. The dataset contained on average 55% high quality CO_2 flux measurements.

Net ecosystem productivity (NEP) was used to describe the negative sign of measured NEE (Kirschbaum et al., 2001; Lovett et al., 2006). Positive values indicate CO_2 uptake by forests whereas negative values indicate CO_2 released to the atmosphere. In order to avoid additional uncertainty introduced by flux partitioning based on night-time ecosystem respiration, we used direct measurements of NEP instead of GPP.

2.4. Data selection

Data analysis was focused on daylight hours (potential global radiation, $R_{pot} > 20$ W m^{-2}) during the summer of 2012 and 2013. The data covered a measurement period from June 19 to September 30, 2012 and from June 1 to September 4, 2013. PAR_t measurements at EC tower and tall tower sites are very similar (R^2 of 0.97) during daylight hours, however we used the EC site PAR measurements which has less scattered data. Diffuse fraction (f_{dif}) is the fractional ratio of the diffuse PAR to the total PAR (Dengel and Grace, 2010; Niyogi et al., 2004; Roderick et al., 2001). The diffuse PAR sensor at the tall tower had offsets of about 3 μmol photon m^{-2} s^{-1}; however, we used the original data without calibration. We replaced f_{dif} with 1 if it exceeded 1. Data points with missing T_a and VPD were discarded. A clearness index (CI) was computed as the ratio between actual global radiation (Rg) and R_{pot}. In this study, CI is the same concept as atmospheric transmittance (Knohl and Baldocchi, 2008) and relative irradiance (Cirino et al., 2014; Oliveira et al., 2007). CI was used to determine the reduction of total incident PAR due to clouds and/or smoke particles.

2.5. Artificial Neural Networks

To characterize the environmental drivers of NEP, we used a methodology based on Artificial Neural Networks (ANNs) developed for ecological datasets (Moffat et al., 2010). ANNs are a data-driven approach just like machine-learning techniques. The hierarchy of environmental controls and functional relationships are identified directly from the half-hourly measurements. During the training process, the correlations and relationships of environmental drivers with the ecosystem response are mapped onto the ANNs.

Fourteen environmental drivers were used as input variables (Table 1) to model the NEP response. The ANNs requires a complete set of input and output drivers. In total, 2542 half-hourly data points were used for ANN training (1089 for 2012, 1453 for 2013).

The ANNs training scenarios consisted of different sets of input variables. First, the ANNs were trained with all fourteen drivers and the potential model performance with all available input drivers was used as a benchmark. Then, the ANNs were trained with one input driver at a time to determine the primary drivers. Finally, the ANNs were trained with the dominant primary driver plus each of other input variables as secondary drivers. Tertiary drivers were identified by fixing both the primary and the secondary drivers. A detailed example of this procedure can be found in Moffat (2012).

Table 1
List of environmental variables used for the ANNs trainings.

NEP	Net ecosystem productivity (μmol CO_2 $m^{-2} s^{-1}$)
PAR_t	Downward total photosynthetically active radiation (μmol photon $m^{-2} s^{-1}$)
PAR_{dir}	Direct PAR (μmol photon $m^{-2} s^{-1}$)
PAR_{dif}	Diffuse PAR (μmol photon $m^{-2} s^{-1}$)
Rg	Global radiation ($W m^{-2}$)
VPD	Vapor pressure deficit (hPa)
RH	Relative humidity (%)
SWC	Soil water content at 0.32 m depth (%)
T_a	Air temperature (°C)
Ts1, Ts2	Soil temperature at 0.04 m and 0.32 m depth (°C)
G	Ground heat flux ($W m^{-2}$)
WD	Wind direction (°)
WS	Horizontal wind speed ($m s^{-1}$)
u_*	Friction velocity ($m s^{-1}$)
f_{dif}	Diffuse fraction

In the next step, the functional relationships of the three most important drivers (PAR_t, VPD, f_{dif}) were extracted from the ANNs. The ANNs trained on the summer data represent a model of the dependence of mean ecosystem behaviour on these three drivers. The sensitivity of the NEP to changes in these environmental drivers under different AOD values was investigated using this the ANNs.

3. Results

3.1. Meteorological conditions and NEP

Mean daily T_a ranged between 8.1 and 27.1 °C in 2012, and between 4.4 and 26.9 °C in 2013 (Fig. 2a). For the periods between June 19 and June 23, the mean daily T_a was about 17.5 °C in both years. During this period, the maximum temperature in 2012 was reached 4 days later than in 2013. T_a for June 2012 (18.1 °C) was warmer and drier than the same period in 2013. T_a reached its peak towards the end of July. Maximum values of VPD (25.3 hPa on 22 July 2012; 22.7 hPa on 17 July 2013) were observed at the same time as the maxima of T_a (Fig. 2a). In both years, both T_a and VPD started to decrease in the middle of August.

From mid-July to the end of August the total rainfall was 28.1 mm in 2012 and about five times higher in 2013 (139.3 mm; Fig. 2b). In the time before the installation of the EC tower in 2012, precipitation was very low as recorded at the neighboring tall tower site with similar soil characteristics resulting in very dry soil conditions compared to 2013. The precipitation average of 5 mm in July 2012 was not enough to increase the low soil moisture contents. Maximum soil water content (SWC) at a depth of 0.32 m was two times higher in 2013 (15.5%) than in 2012 (8.6%).

Mean daily PAR_t in 2012 (350.0 μmol $m^{-2} s^{-1}$) was about 50 μmol $m^{-2} s^{-1}$ lower than in 2013 (400.3 μmol $m^{-2} s^{-1}$), whereas the maximum value of about 625 μmol $m^{-2} s^{-1}$ in 2013 was

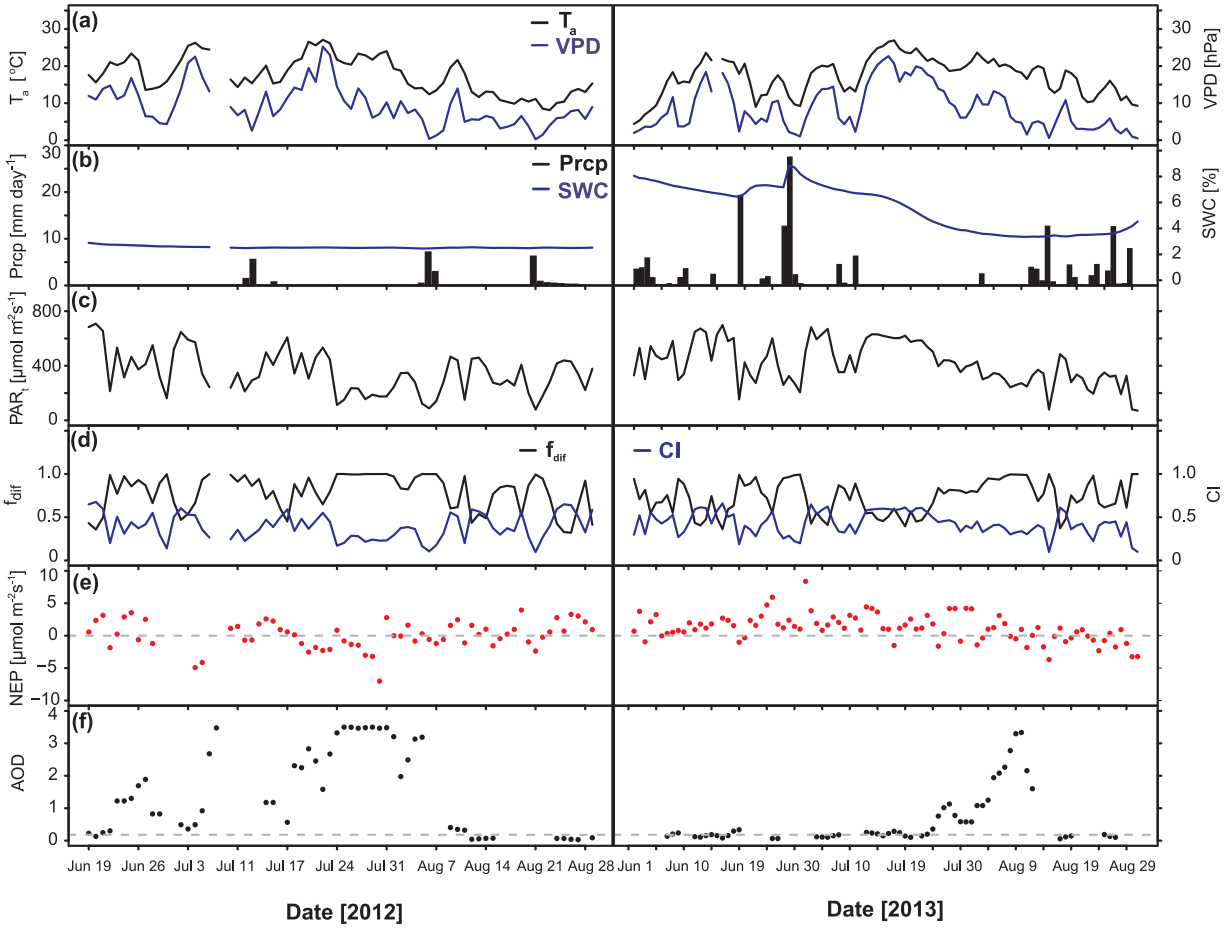

Fig. 2. Time series of daily observation at ZOTTO. (a) Air temperature (T_a, black), vapor pressure deficit (VPD, blue), (b) total precipitation (Prcp, black), soil moisture at 0.32 m (SWC, blue), (c) total incident photosynthetic active radiation (PAR_t), (d) diffuse fraction (f_{dif}, black), clearness index (CI, blue), (e) net ecosystem productivity (NEP, red), and (f) AOD from June 19 to September 4, 2012 (left) and June 1 to September 4, 2013 (right). Only f_{dif} and CI are averaged in daylight hours ($R_{pot} > 20 W m^{-2}$). The horizontal grey dashed line of (f) is the mean background AOD value of 0.18 during June–August in Siberia (Remer et al., 2008). (For interpretation of the references to colour in this figure legend, the reader is referred to the web version of this article.)

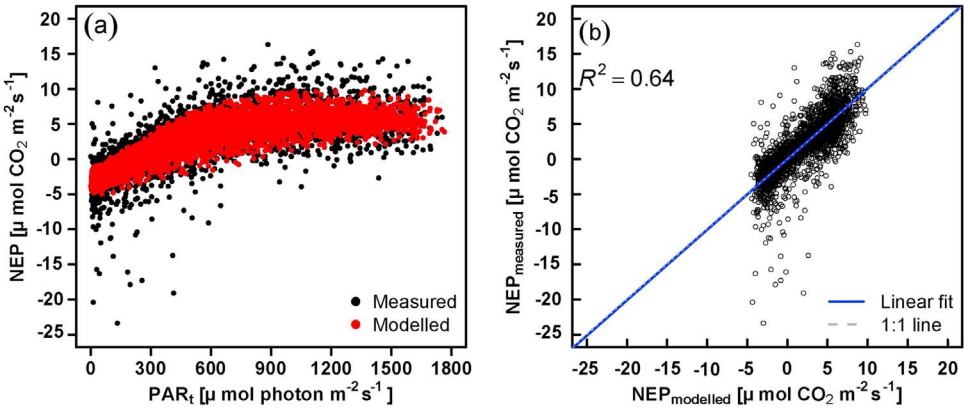

Fig. 3. Results of the ANN benchmarked with all fourteen environmental drivers: (a) Measured (black) and modelled (red) daytime NEP response projected onto PAR_t. (b) Scatterplot of measured versus modelled daytime NEP. The linear regression fit (blue solid line) is close to the 1:1 line (grey dashed line). Positive NEP values indicate CO_2 uptake by forests whereas negative values indicate CO_2 released to the atmosphere. See Table 1 for details on the environmental drivers. (For interpretation of the references to colour in this figure legend, the reader is referred to the web version of this article.)

25.4 μmol $m^{-2} s^{-1}$ higher than in 2012 (600 μmol $m^{-2} s^{-1}$). The averaged maximum daily PAR_t in both years was similar at about 700 μmol $m^{-2} s^{-1}$. A daily averaged CI of 0.42 during daylight hours indicates that the conditions at the study site were mostly cloudy or overcast in both years.

Daily NEP varied between −7.00 and 3.38 μmol CO_2 $m^{-2} s^{-1}$ in 2012, whereas it fell between −3.68 and 8.38 μmol CO_2 $m^{-2} s^{-1}$ in 2013. The daily averaged NEP reached a minimum of 3.54 μmol CO_2 $m^{-2} s^{-1}$ on the 25th of June 2012. Monthly averaged NEP was −0.55 μmol CO_2 $m^{-2} s^{-1}$ in July of 2012 and 1.88 μmol CO_2 $m^{-2} s^{-1}$ in July of 2013. The situation for August was the opposite, with NEP of 0.66 μmol CO_2 $m^{-2} s^{-1}$ in 2012 and −0.44 μmol CO_2 $m^{-2} s^{-1}$ in 2013.

3.2. Wildfire

In general, fires in central Siberia occur between July and late August (Valendik et al., 2014). However, in 2012 they started already in late June and lasted until the first week of August. Summer of 2012 was recorded as a mega-fire in Siberia due to a stable anticyclone that result in high temperatures and low precipitation (Zhuravleva et al., 2017). In 2012, about 83% of the surface area (7111 km^2) in a 100 km radius around ZOTTO burned (Antamoshkina and Korets, 2015). During the 2000–2014 period, the highest fire occurrences (33 fire events) were in lichen forests within a 100 km radius around the ZOTTO site. Conversely, in 2013, the burnt area was the 5th largest (237 km^2) fire in this period, and the fire season was less active (8 fire events) than in 2012.

We used AOD as a smoke aerosol proxy, which revealed that the aerosol particle number concentrations increased along with the atmospheric carbon monoxide (CO) concentration, in agreement with previous observations (Chi et al., 2013). We observed overall phasing and similar amplitudes of AOD and CO mixing ratio (not shown) similar to those observed by Konovalov et al. (2014), suggesting that our use of AOD is an appropriate indicator of fire emissions during these periods. Hence, we assumed that AOD is mainly driven by smoke from fire. At ZOTTO, for the period from June to August in 2012 and 2013, the daily

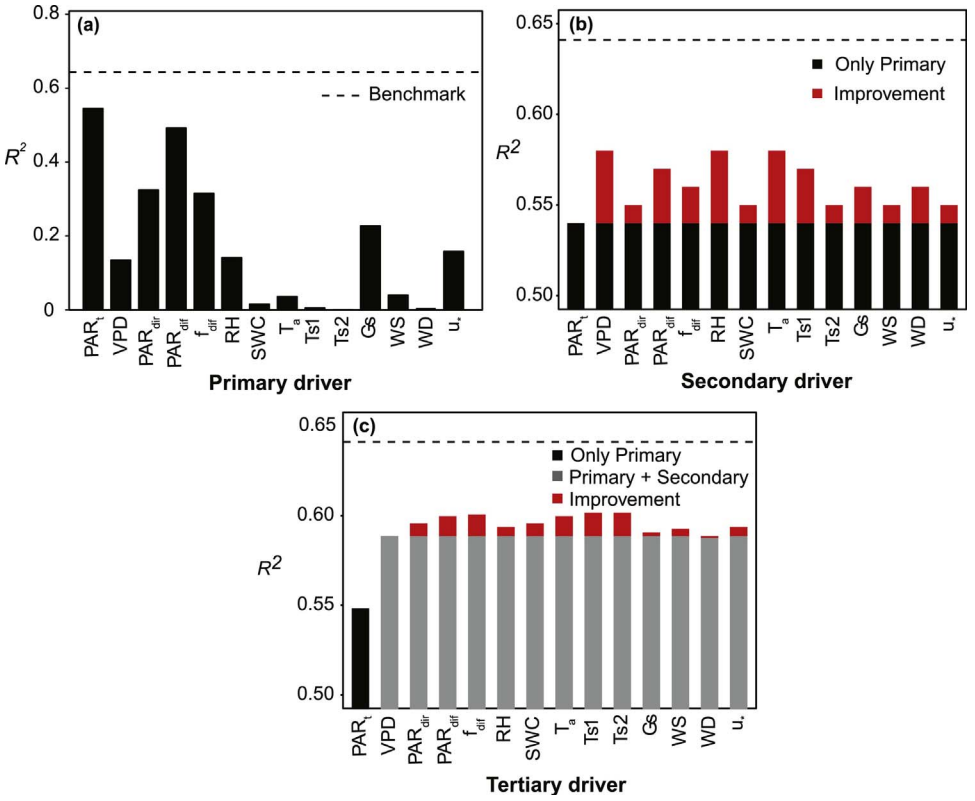

Fig. 4. Performance (R^2) of the ANNs trained with 14 input drivers: (a) with a single (primary) driver at a time, (b) with PAR_t plus a secondary driver, and (c) with PAR_t and VPD plus a tertiary driver. The performance improvement (red) indicates the relevance of the secondary and tertiary drivers. The horizontal dotted line is the benchmark performance with all 14 drivers. (For interpretation of the references to colour in this figure legend, the reader is referred to the web version of this article.)

MODIS AOD was available in total for 85 days. The maximum baseline AOD (2007–2011) was 0.95 and the present AOD in 2012–2013 was 3.5.

3.3. Drivers of NEP

The benchmark ANN trained with all 14 drivers indicated that modelled NEP generally agrees well with observation, but with lower variability (Fig. 3a). The coefficient of determination (R^2) was 0.64 with a standard deviation of the model residuals of ± 2.58 µmol CO_2 $m^{-2}s^{-1}$ (Fig. 3b).

The analysis of the hierarchy of the environmental drivers identified PAR_t as the dominant primary driver, VPD as the main secondary driver, and soil temperatures at 0.08 and 0.32 m depth (Ts1 and Ts2) or f_{dif} as tertiary drivers (Fig. 4). For ANNs trained with single drivers (Fig. 4a), PAR_t had a higher model performance (R^2 of 0.54) than any of the other radiative drivers (*e.g.*, R^2 of 0.53 for Rg, 0.32 for PAR_{dir}, and 0.49 for PAR_{dif}). Adding VPD explained an additional ~4% of the variability (R^2 of 0.59, Fig. 4b). VPD is calculated from RH and T_a, which have similar relevance as secondary drivers. Including f_{dif} as a tertiary driver explains about 2% of the additional variability of NEP (R^2 of 0.60), and allows us to approach the benchmark of 0.64 (Fig. 4c). The importance of Ts1 and Ts2 is similar to that of f_{dif}. All other environmental variables showed smaller improvements as tertiary drivers. The influence of the micrometeorological variables (WS, WD, and u_*) was only marginal, which is expected for a cleaned dataset.

The ANNs trained with the three main drivers (PAR_t, VPD and f_{dif}) can be used to analyze the functional relationships between these drivers and NEP. Light response shows the expected behaviour (Fig. 5a): for low light, the partial derivative of NEP with PAR_t (*i.e.*, LUE), is constantly around 0.015 µmol CO_2/µmol photons, translating to an almost linear slope in the beginning at low values of PAR_t. NEP values are negative (indicating respiration) around −3 µmol CO_2 $m^{-2}s^{-1}$. At higher levels of PAR_t, the NEP response levels off, saturating with the derivative approaching zero and optimum NEP values around +6 µmol CO_2 $m^{-2}s^{-1}$.

The NEP response exhibits a decrease (negative derivative) with increasing air dryness over the entire range of VPD (Fig. 5b). The partial derivative of NEP with f_{dif} is positive over the full range of f_{dif} values, indicating a positive effect of diffuse light on NEP (Fig. 5c).

3.4. How do clouds and smoke affect the partitioning of PAR?

Both f_{dif} and CI describe the behaviour of the light intensity due to clouds and smoke particles (Fig. 6a). Overall, 75.4% of half-hourly data where $f_{dif} > 0.3$ are influenced by clouds and smoke particles. A linear negative relationship between CI and f_{dif} exists for f_{dif} values lower than 0.95. If CI is lower than 0.5, f_{dif} saturates to 1, indicating a reduction of incoming PAR due to thick clouds (overcast conditions) or very thick smoke. Incoming PAR shows a strong and significant ($p < 0.001$) negative correlation with f_{dif}, indicating an increase PAR_t with clearer skies (Fig. 6b). The relationship between PAR_{dif} and f_{dif} is nonlinear; PAR_{dif} increases with f_{dif}, reaching its maximum at around $f_{dif} = 0.9$, then decreases at higher values of f_{dif}.

We observed a significant reduction of incoming PAR due to AOD, whereas PAR_{dif} first increases up to a critical value due to the aerosol scattering effect, then decreases at high levels of smoke intensity due to reduced PAR_t (Fig. 7a). The relationships between PAR_t and f_{dif} and between PAR_t and AOD are strong and significant. In general, f_{dif} increase with AOD, but it saturates to 1 at values of AOD greater than 2 (Fig. 7b). Overall, AOD explains about 76% of variability in f_{dif}, but with large scatter at low AOD, indicating an additional influence of clouds. Values of $f_{dif} > 0.3$ are seen on cloudy or overcast days, showing the influence of clouds at low smoke conditions.

3.5. How relevant is the effect of smoke on NEP?

We performed a sensitivity analysis to predict the normalized midday mean NEP during summer using data on changes in meteorological drivers (Table 2). Overall, reductions in PAR_t have a much greater impact on NEP than increases in f_{dif}. Reductions of 10–30% in PAR_t decreased normalized midday mean NEP compared with the measured NEP. Increases in NEP are also caused by f_{dif} but only if PAR_t reduction is not more than 20%.

An increase in f_{dif} of 150% increases NEP ~20%, whereas a reduction in PAR_t of 60% decreases NEP ~24%. No scenarios that we tested (increases in f_{dif} up to 150%) increased NEP when PAR_t was reduced by 30% or more.

Theoretically, without reduction in PAR_t, NEP increases from 4 to

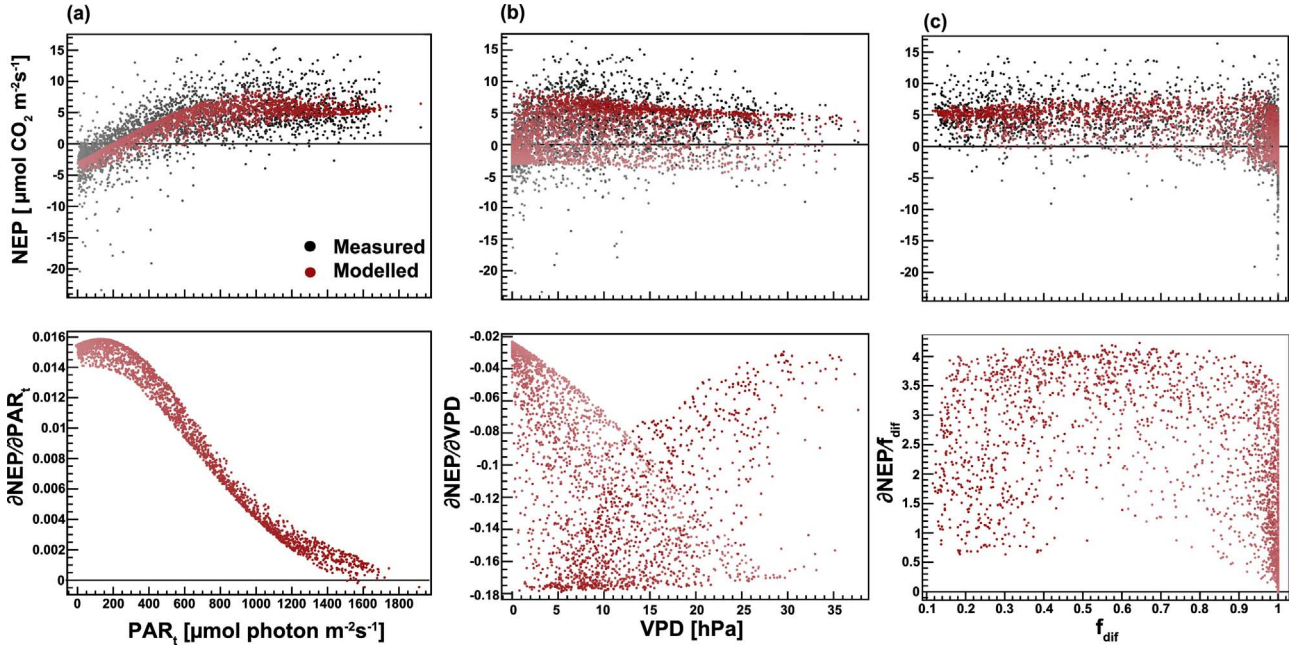

Fig. 5. Daytime NEP response (upper panel) and partial derivatives (lower panel) modelled with three drivers PAR_t (a), VPD (b), and f_{dif} (c). The modelled (red circles) and measured (black circles) NEP values are shown in gradient colours from light to dark denoting low to high PAR_t. (For interpretation of the references to colour in this figure legend, the reader is referred to the web version of this article.)

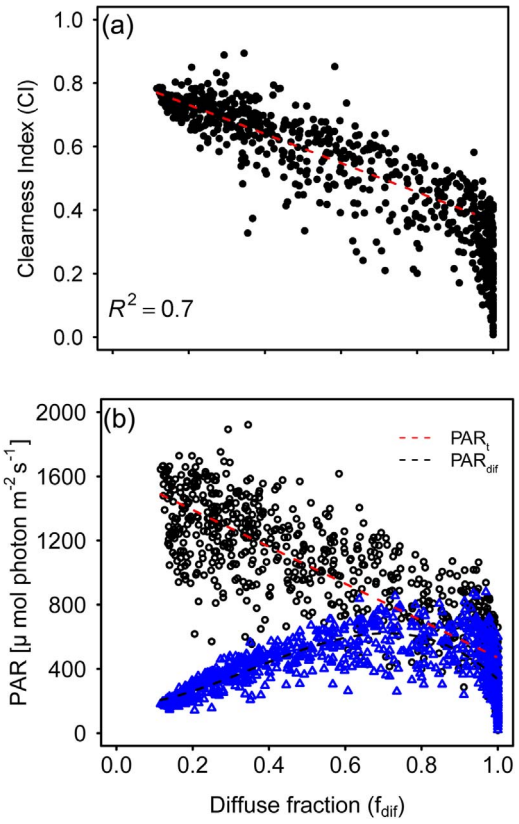

Fig. 6. (a) Relationship between proportion of diffuse to total PAR (f_{dif}) and clearness index (CI) at midday (11:00-15:00) in summer (Linear fit [red dashed line] of $f_{dif} < 0.95$; CI = 0.82 − 0.46*f_{dif}, $R^2 = 0.70$, $p < 0.001$, n = 539), and (b) between f_{dif} and total (black circles) and diffuse (blue triangles) PAR. Linear fit (red dashed line) of total PAR (PAR_t = 1652.11–1154.17 *f_{dif}, $R^2 = 0.75$, *p-value* < 0.001) and 3rd polynomial fit (black dashed line) of PAR_{dif} (PAR_{dif} = 172.99 + 44.74 *f_{dif} + 2637.56 *$(f_{dif})^2$ − 2502.92*$(f_{dif})^3$, $R^2 = 0.56$, p < 0.001, n = 730). (For interpretation of the references to colour in this figure legend, the reader is referred to the web version of this article.)

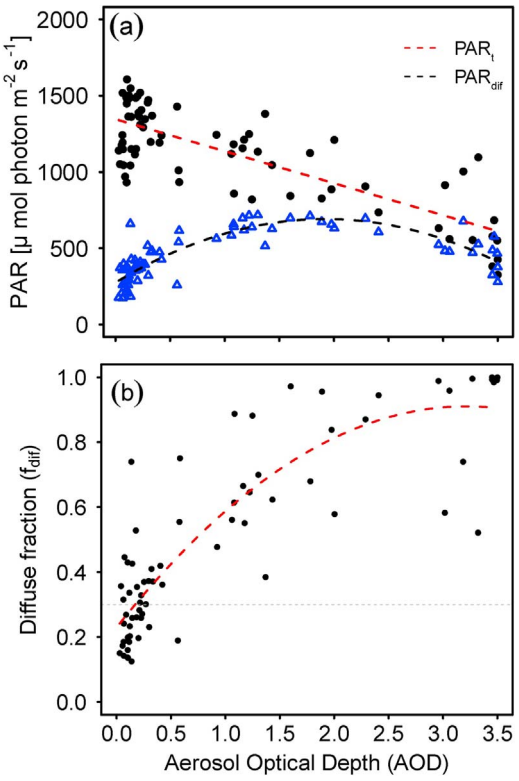

Fig. 7. (a) Relationship between daily AOD and PAR components and (b) between a fraction of diffuse PAR at midday (11:00-15:00) in summer. Black circles and blue triangles denote PAR_t and PAR_{dif}, respectively. The linear fit of PAR_t (red dashed line) of (a) is PAR_t = 1345.92–209.89*AOD, $R^2 = 0.64$, *p-value* < 0.001, the 2nd polynomial fit of PAR_{dif} = 275.53 + 433.05*AOD − 112.74*$(AOD)^2$, $R^2 = 0.71$, *p-value* < 0.001. The 2nd polynomial fit of f_{dif} and AOD is f_{dif} = 0.23 + 0.43*(AOD) − 0.07*$(AOD)^2$, R^2 = 0.76, *p-value* < 0.001). The total sample size is 72. The grey dashed line at $f_{dif} = 0.3$ indicates a threshold of clear sky conditions. (For interpretation of the references to colour in this figure legend, the reader is referred to the web version of this article.)

37% due to the f_{dif} enhancement (up to 400%). Conversely, NEP would decrease from 6 to 83% due to reductions in PAR_t ~60%. However, actual NEP responds differently due to the compensation of PAR_t for f_{dif} and vice versa For instance, a forest experiencing a 10% reduction in PAR_t and a 50% increase in f_{dif} is predicted to be 2% less productive compared with the measured NEP. However a forest experiencing the same reduction in PAR_t and 100–400% increase in f_{dif} is predicted to be 2–33% more productive compared with the measured NEP. When PAR_t is reduced by 15%, NEP enhancement requires an increase in f_{dif} greater than 150%. When PAR_t is reduced by 40%, NEP enhancement requires an increase in f_{dif} greater than 350% (corresponding to PAR_t = 959.6 μmol photon m^{-2} s^{-1} and f_{dif} of 0.9). When PAR_t is reduced by 50%, no increase in f_{dif} is sufficient to sustain forest productivity.

Overall, the decrease in PAR_t overwhelms the increase in f_{dif} caused by high AOD during fires. At low to moderate levels of AOD (0.3–1), forests experiencing a 7–11% reduction in PAR_t and a 41–67% increase in f_{dif} resulting in a 1.45% increase in NEP. However, at higher levels of AOD (2–3.5), NEP decreases about 7% due to a 28% reduction in PAR_t and despite a 132% increase in f_{dif}. This is most pronounced at the maximum AOD of 3.5 during fires, which results in a ~42% reduction in NEP due to a 52% reduction in PAR_t and despite an increase in f_{dif} up to 158%.

4. Discussion

4.1. Environmental drivers of NEP identified by the ANNs

We can explain 60% of the benchmark of 64% variation in NEP using data on PAR_t, VPD, and f_{dif} or soil temperatures. Light intensity, VPD, and T_a are known to be key controls of photosynthesis (Goulden et al., 1997; Jarvis et al., 1997; Chen et al., 2002). A wide range of VPD implies that water vapor quickly evaporates due to the strong influence of air dryness (Figs. 2 and 5b). With the optimum temperature range for evergreen coniferous trees of 10–25 °C (Larcher, 2003), an increase in VPD at water-limited sites causes a reduction in productivity because of the closing of stomata to prevent water loss (Fig. 5b, Dengel and Grace, 2010; Kelliher et al., 1997; Lloyd et al., 2002; Shibistova et al., 2002). At VPD above 10 hPa, the stomata begin to close, thus reducing photosynthesis and transpiration rates in boreal trees (Dang et al., 1997; Hogg and Hurdle, 1997).

In general, temperature controls the distinct seasonality of photosynthesis and respiration rates (Lloyd et al., 2002). Due to the tight coupling between temperature and humidity, temperature sensitivity may have similar down-regulating effects as VPD. Similar to Alton et al. (2007), stomata might not be fully open at high humidity conditions (low VPD) if the light intensity is too low for photosynthesis.

When light is saturated, NEP can be interpreted as a proxy for, but not equal to, the ecosystem photosynthetic capacity (Musavi et al., 2016; Reichstein et al., 2014). Light responses (Fig. 3b) show that an ecosystem at high northern latitudes quickly reaches the light saturation point. For instance, NEP in tropical forests reaches its maximum saturation when PAR_t is around 1550–1870 μmol m^{-2} s^{-1} (Cirino et al., 2014), whereas in the ZOTTO forest, the maximum NEP is reached when PAR_t is around 700–900 μmol m^{-2} s^{-1}.

Table 2
Midday (11:00–15:00) normalized mean NEP during summer was estimated by considering the percentage decreases and increases in PAR_t and f_{dif}. VPD variation is fixed. All values are percentage changes in NEP relative to our measured midday mean NEP during summer. Zero is the measured NEP with no change in meteorology. We simulated 10–60% decreases in PAR_t by increasing f_{dif} from 50 to 400%. Corresponding PAR_t values for the relative changes decrease 10–60% from 1400 to 600 μmol photon $m^{-2} s^{-1}$ at a rate of 100 μmol photon $m^{-2} s^{-1}$ (Fig. 6b). In the same manner, relative increases from 0.2 to 1 in f_{dif} range from 50 to 400% in increments of 0.1. The first column indicates NEP considering the reduction of PAR_t, while the first row indicates NEP only considering the f_{dif} increase. Increasing AOD from 0.3 to 0.7, 1, 1.5, 2, and 3.5, the relative changes in PAR_t decrease by about 7, 11.5, 19.6, 27.8, and 52.4%, respectively (Fig. 7a). Similarly, the relative increases in f_{dif} from 50 to 200% with AOD are 41, 67.5, 104.5, 132, 158.3%, respectively (Fig. 7b). The thick bold line indicates the line between negative and positive effects due to PAR_t and f_{dif} changes.

NEP change [%]		f_{dif} changes								
		0%	+50%	+100%	+150%	+200%	+250%	+300%	+350%	+400%
PAR_t changes	0%	0	3.6	7.5	11.8	16.4	21.2	26.3	31.6	37.0
	-10%	-5.7	**-1.8**[1)]	**2.3**[2)]	6.8	11.6	16.7	21.8	27.2	32.7
	-15%	-9.4	-5.5	-1.2	3.4	8.3	13.4	18.6	24.1	29.6
	-20%	-13.9	-9.8	**-5.4**[3)]	-0.7	4.2	9.4	14.7	20.1	25.6
	-35%	-32.0	-27.6	-23.0	**-18.1**[4)]	-13.0	-7.8	-2.4	2.0	8.3
	-40%	-40.0	-35.5	-30.8	-25.9	-20.8	-15.5	-10.2	-4.9	0.4
	-50%	-60.0	-54.7	-49.9	**-44.9**[5)]	-39.8	-34.6	-29.4	-24.2	-19.2
	-60%	-83.3	-78.7	-73.8	-68.8	-63.7	-58.7	-53.6	-48.7	-44.0

Values are obtained from Fig. 7.
1): NEP where AOD increases from 0.3 to 0.7, decreasing PAR_t 7% (1198.0 μmol photon $m^{-2} s^{-1}$) and increasing f_{dif} 41% (0.49).
2): NEP where AOD increases from 0.3 to 1, decreasing PAR_t 11.5% (1136.03 μmol photon $m^{-2} s^{-1}$) and increasing f_{dif} 67.5% (0.59).
3): NEP where AOD increases from 0.3 to 1.5, decreasing PAR_t 19.6% (1031.09 μmol photon $m^{-2} s^{-1}$) and increasing f_{dif} 104.5% (0.72).
4): NEP where AOD increases from 0.3 to 2, decreasing PAR_t 27.8% (926.14 μmol photon $m^{-2} s^{-1}$) and increasing f_{dif} 132% (0.81).
5): NEP where AOD increases from 0.3 to 3.5, decreasing PAR_t 52.40% (611.31 μmol photon $m^{-2} s^{-1}$) and increasing f_{dif} 158.37% (0.91).

4.2. Effects of clouds and smoke on radiation

Incoming PAR decreases significantly at very high levels of f_{dif} and AOD (Figs. 6 and 7). A similar correlation between f_{dif} and CI (Fig. 6a) is also found at other sites (Knohl and Baldocchi, 2008; Roderick et al., 2001), although the ZOTTO site has a higher CI regime (~0.45) compared to other sites (~0.2). Diffuse PAR and f_{dif} are values defined at wavelengths relevant for photosynthesis, whereas the definition of CI includes a wider range of wavelengths. Using CI may have more confounding effects or overestimate the influence of clouds and aerosols on ecosystem responses (Cohan et al., 2002; Kanniah et al., 2010; Letts et al., 2005).

Clouds play a more significant role in determining PAR_t than AOD (Figs. 6b, 7a), as found in modelling studies (Min, 2005; Schafer et al., 2002b). However, the separation of a reduction in PAR_t caused by aerosol effect and that caused by clouds is not possible (Cirino et al., 2014).

An increase of PAR_{dif} and f_{dif} with increase in AOD up to ~2, and a decrease of both parameters at higher AOD values (Fig. 7) are consistent with previous studies (Cirino et al., 2014; Jing et al., 2010; Kanniah et al., 2010; Min, 2005; Moon et al., 2009; Oliphant et al., 2011; Oliveira et al., 2007; Schafer et al., 2002b; Steiner et al., 2013; Strada et al., 2015). The peak of PAR_{dif} at values of f_{dif} around 0.9 (Fig. 6b) may be due to the fact that on overcast days more light is scattered than on days with more patchy cloud cover (Cohan et al., 2002; Min, 2005). Large scatter of f_{dif} during low smoke (AOD < 0.3) conditions implies that cloud effects on f_{dif} may play a role in the DRF effect (Fig. 7b). Previous studies have shown that a moderate level of f_{dif} is predominately caused by aerosols or thin clouds, although the effects of the two are confounded (Min, 2005; Oliphant et al., 2011).

The size distribution and concentration of water vapor droplets in clouds depends on the types of aerosols present, changing cloud microphysics and radiative fluxes. For instance, clouds induced by smoke particles embrace more and smaller size water droplets compared to smoke-free clouds under the same conditions, leading to an increase in cloud cover of up to 5% (Kaufman and Koren, 2006). Also, MODIS AOD is known to be overestimated at 550 nm (Levy et al., 2010). Several studies have shown that fine resolution ground-based aerosol measurements (*e.g.*, size distribution, light scattering coefficients, AOD) help to understand the role of smoke particles on clouds and the radiation budget (Oliphant et al., 2011; Yamasoe et al., 2006). However, the influence of AOD on incoming radiation may not be as pronounced as that of clouds because it responds indirectly to photosynthesis (Figs. 6 and 7). An insignificant relationship between NEP and AOD supports this hypothesis (not shown). In other words: as shown by ANNs analysis, the environmental drivers PAR_t, VPD, and f_{dif} play a more important role than AOD in explaining NEP (Fig. 4). Therefore, the predicting NEP without AOD as a training driver of ANNs is appropriate.

Maximum NEP enhancement occurs when PAR_{dif} reaches its maximum (638.2 μmol photon $m^{-2} s^{-1}$) at f_{dif} of 0.7. However, at this light level, PAR_t is 844.2 μmol photon $m^{-2} s^{-1}$ lower than the maximum value with no cloud cover (Figs. 7b and 4a). The forest ecosystem is still productive under low light conditions, because of the NEP increase caused by increasing f_{dif} (Fig. 4c); however, the relative change in NEP is less than ~10% (Table 2). Moreover, at very large AOD values (> 2), we found that NEP is reduced by 50% due to the strong reduction of PAR_t although separating the effect of clouds and smoke on this reduction is not possible (Cirino et al., 2014).

4.3. Requirements of the diffuse radiation fertilization (DRF) effect

Our sensitivity analysis showed that a DRF effect in the ZOTTO forest is theoretically possible, but that it is not often observed due to the overall strong reduction in PAR_t by clouds and smoke (Table 2). One possible explanation of why the DRF effect at our site is not as pronounced as in other forests (Doughty et al., 2010; Knohl and Baldocchi, 2008; Mercado et al., 2009; Niyogi et al., 2004; Oliveira et al., 2007; Rap et al., 2015; Still et al., 2009; Yamasoe et al., 2006) might be the sparse canopy and the low LAI. Our results also provide evidence that within the same PFT, the DRF effect is not as pronounced in forests with lower LAI (Gu et al., 2002).

Kanniah et al. (2012) concluded that ecosystems with low LAI may not experience positive effects of diffuse light on vegetation

productivity. This is particularly true in open canopy ecosystems, such as grasslands (Niyogi et al., 2004; Wohlfahrt et al., 2008) and wetlands (Letts et al., 2005). A simulation using a multi-layer canopy model showed that the DRF effect decreases with decreasing LAI and it also depends on leaf clumping and leaf angle (Knohl and Baldocchi, 2008). However, substantial increase of CO_2 uptake due to thick clouds were found in a grassland with very low LAI (~ 0.37; Jing et al., 2010) as well as in some forests with low LAI (~ 2; Migliavacca et al., 2009; Misson et al., 2005). Observations in multi-layered arctic shrub ecosystems with low LAI (~1.5) support our argument that the importance of canopy structure on DRF effects is independent from of LAI (Williams et al., 2014). Therefore, we argue that canopy structure may be a more crucial factor than LAI in determining DRF effects.

In our Siberian forest at very high levels of AOD (> 3), both PAR_t and PAR_{dif} are ~700 μmol photon $m^{-2} s^{-1}$ and f_{dif} is high (> 0.6; Fig. 7). High f_{dif} can be caused by both overcast conditions (thick clouds) or by the presence of smoke (Figs. 6b, 7b). Although it is not possible to separate smoke from cloud effects, higher aerosol loading and thick cloud cover have a large impact on forest NEP by changing the amount of incoming PAR reaching the surface (Oliveria et al., 2007; Cirino et al., 2014). A possible explanation for a strong reduction of PAR_t may be to the fact that smoke absorbs solar radiation and suppresses the formation of clouds (Andreae et al., 2004; Koren et al., 2004). Our results support those of Alton (2008), namely that increases ecosystem productivity due to diffuse radiation are less than 10%.

5. Conclusion

Due to increased drying and warming, the Siberian taiga is increasingly exposed to fires. However, the ecosystem NEP response may be non-linear depending on the complex interaction among clouds and aerosol types, canopy structure, the magnitude of fires, and associated meteorological conditions. Here, we combine eddy covariance flux measurements and data-driven modelling in order to understand the environmental drivers of forest NEP and investigate the impact of smoke and clouds on diffuse and direct components of radiation partitioning.

The ANNs analysis suggest that the f_{dif} did increase NEP, however, it was more sensitive to a strong reduction of PAR_t than to diffuse light enrichment due to clouds or high smoke. The overall effect of a potential increase in NEP due to thick clouds or high aerosol loading minimized by the low light intensity, sparse canopy structure and low LAI. The ANNs have the benefit of quantifying the impact of diffuse radiation on NEP without additional canopy structure parameters. This represents an important advance in understanding ecosystem functional properties and their effects on photosynthesis. Moving forward, our results suggest that, in the particular case of sparse canopies with low LAI (e.g., grasslands and wetlands), the DRF effect should be included in biogeochemical models and coupled Earth System models in order to better describe net ecosystem productivity.

Acknowledgements

The ZOTTO project is funded by the Max Planck Society through the International Science and Technology Center (ISTC) partner project no. 2757 within the framework of the proposal “Observing and Understanding Biogeochemical Responses to Rapid Climate Changes in Eurasia”. We would like to thank the technical staff (Karl Kübler, Steffen Schmidt, and Martin Hertel) from the Max Planck Institute for Biogeochemistry in Jena for maintaining the ZOTTO station and setting up the eddy covariance flux tower. For maintaining the flux tower, we deeply appreciate the work of Dr. Alexey Panov, Alexander Zukanov, Nikita Sidenko, Sergey Titov, and Anastasiya Timokhina from the V.N. Sukachev Institute of Forest in Krasnoyarsk, and many other supporters in Zotino. We also thank Dr. Yuanchao Fan and Dr. Ingo Schöning for their constructive comments on the draft. Special thanks go to Emily Zeran and Dr. Andrew Durso for the proof reading and Mikhail Urbazaev and Yu Okamura for assisting in preparation of Figs. 1, 4, and 5. A. Prokushkin is supported by grant RSF #14-24-00113. S.-B. Park acknowledges the International Max Planck Research School for Global Biogeochemical Cycles (IMPRS-gBGC). We greatly appreciate the reviewers’ comments and suggestions.

References

Achard, F., Eva, H.D., Mollicone, D., Beuchle, R., 2008. The effect of climate anomalies and human ignition factor on wildfires in Russian boreal forests. Philos. Trans. R. Soc. Lond. B. Biol. Sci. 363, 2331–2339. http://dx.doi.org/10.1098/rstb.2007.2203.

Alton, P.B., North, P., Kaduk, J., Los, S., 2005. Radiative transfer modeling of direct and diffuse sunlight in a Siberian pine forest. J. Geophys. Res. Atmos. 110, D23209. http://dx.doi.org/10.1029/2005JD006060.

Alton, P.B., North, P.R., Los, S.O., 2007. The impact of diffuse sunlight on canopy light-use efficiency, gross photosynthetic product and net ecosystem exchange in three forest biomes. Glob. Change Biol. 13, 776–787. http://dx.doi.org/10.1111/j.1365-2486.2007.01316.x.

Alton, P.B., 2008. Reduced carbon sequestration in terrestrial ecosystems under overcast skies compared to clear skies. Agric. For. Meteorol. 148, 1641–1653. http://dx.doi.org/10.1016/j.agrformet.2008.05.014.

Andreae, M.O., Rosenfeld, D., Artaxo, P., Costa, A.A., Frank, G.P., Longo, K.M., Silva-Dias, M.A.F., 2004. Smoking rain clouds over the amazon. Science 303, 1337–1342. http://dx.doi.org/10.1126/science.1092779.

Antamoshkina, O.A., Korets, M.A., 2015. Vegetation monitoring within the ZOTTO tall tower coverage area using remote sensing data. Vestnik SibGAU 16 (4), 814–818 (In Russian).

Arneth, A., Lloyd, J., Shibistova, O., Sogachev, A., Kolle, O., 2006. Spring in the boreal environment: observations on pre- and post-melt energy and CO_2 fluxes in two central Siberian ecosystems. Boreal Environ. Res. 11, 311–328.

Chen, J.Q., Falk, M., Euskirchen, E., Suchanek, T.H., Ustin, S.L., Bond, B.J., Brosofske, K.D., Phillips, N., Bi, R.C., 2002. Biophysical controls of carbon flows in three successional Douglas-fir stands based on eddy-covariance measurements. Tree Physiol. 22, 169–177.

Cheng, S.J., Bohrer, G., Steiner, A.L., Hollinger, D.Y., Suyker, A., Phillips, R.P., Nadelhoffer, K.J., 2015. Variations in the influence of diffuse light on gross primary productivity in temperate ecosystems. Agric. For. Meteorol. 201, 98–110. http://dx.doi.org/10.1016/j.agrformet.2014.11.002.

Chi, X., Winderlich, J., Mayer, J.C., Panov, A.V., Heimann, M., Birmili, W., Heintzenberg, J., Cheng, Y., Andreae, M.O., 2013. Long-term measurements of aerosol and carbon monoxide at the ZOTTO tall tower to characterize polluted and pristine air in the Siberian taiga. Atmos. Chem. Phys. 13, 12271–12298. http://dx.doi.org/10.5194/acp-13-12271-2013.

Choudhury, B.J., 2001. Estimating gross photosynthesis using satellite and ancillary data: approach and preliminary results. Remote Sens. Environ. 75, 1–21. http://dx.doi.org/10.1016/S0034-4257(00)00151-6.

Cirino, G.G., Souza, R.A.F., Adams, D.K., Artaxo, P., 2014. The effect of atmospheric aerosol particles and clouds on net ecosystem exchange in the Amazon. Atmos. Chem. Phys. 14, 6523–6543. http://dx.doi.org/10.5194/acp-14-6523-2014.

Cohan, D.S., Xu, J., Greenwald, R., Bergin, M.H., Chameides, W.L., 2002. Impact of atmospheric aerosol light scattering and absorption on terrestrial net primary productivity. Glob. Biogeochem. Cycles 16 (4), 1090. http://dx.doi.org/10.1029/2001GB001441.

Dengel, S., Grace, J., 2010. Carbon dioxide exchange and canopy conductance of two coniferous forests under various sky conditions. Oecologia 164, 797–808. http://dx.doi.org/10.1007/s00442-010-1687-0.

Dengel, S., Grace, J., MacArthur, A., 2015. Transmissivity of solar radiation within a Picea sitchensis stand under various sky conditions. Biogeosciences 12, 4195–4207. http://dx.doi.org/10.5194/bg-12-4195-2015.

Dang, Q.L., Margolis, H.A., Coyea, M.R., Sy, M., Collatz, G.J., 1997. Regulation of branch-level gas exchange of boreal trees: roles of shoot water potential and vapour pressure difference. Tree Physiol. 17, 521–535.

Doughty, C.E., Flanner, M.G., Goulden, M.L., 2010. Effect of smoke on subcanopy shaded light, canopy temperature, and carbon dioxide uptake in an Amazon rainforest. Glob. Biogeochem. Cycles 24, GB3015. http://dx.doi.org/10.1029/2009GB003670.

Foken, Th., Wichura, B., 1996. Tools for quality assessment of surface-based flux measurements. Agric. For. Meteorol. 78, 83–105. http://dx.doi.org/10.1016/0168-1923(95)02248-1.

Forkel, M., Carvalhais, N., Rödenbeck, C., Keeling, R., Heimann, M., Thonicke, K., Zaehle, S., Reichstein, M., 2016. Enhanced seasonal CO_2 exchange caused by amplified plant productivity in northern ecosystems. Science 351, 696–699. http://dx.doi.org/10.1126/science.aac4971.

Furyaev, V.V., Vaganov, E.A., Thebakova, N.M., Valendik, E.N., 2001. Effects of fire and climate on successions and structural changes in the Siberian boreal forest. Eurasian J. For. Res. 2, 1–15.

Goulden, M.L., Daube, B.C., Fan, S.-M., Sutton, D.J., Bazzaz, A., Munger, J.W., Wofsy, S.C., 1997. Physiological responses of a black spruce forest to weather. J. Geophys. Res. 102, 28987–28996. http://dx.doi.org/10.1029/97JD01111.

Gu, L., Shugart, H.H., Fuentes, J.D., Black, T.A., Shewchuk, S.R., 1999. Micrometeorology, biophysical exchanges and NEE decomposition in a two-story boreal forest — development and test of an integrated model. Agric. For. Meteorol. 94, 123–148. http://dx.doi.org/10.1016/S0168-1923(99)00006-4.

Gu, L., Baldocchi, D., Verma, S.B., Black, T.A., Vesala, T., Falge, E.M., Dowty, P.R., 2002. Advantages of diffuse radiation for terrestrial ecosystem productivity. J. Geophys. Res. D Atmos. 107, 4050. http://dx.doi.org/10.1029/2001JD001242.

Gu, L., Baldocchi, D.D., Wofsy, S.C., Munger, J.W., Michalsky, J.J., Urbanski, S.P., Boden, T.A., 2003. Response of a deciduous forest to the Mount Pinatubo eruption: enhanced photosynthesis. Science 299, 2035–2038. http://dx.doi.org/10.1126/science.1078366.

Heimann, M., Schulze, E.-D., Winderlich, J., Andreae, M.O., Chi, X., Gerbig, C., Kolle, O., Kuebler, K., Lavrič, J.V., Mikhailov, E., Panov, A., Park, S., Rödenbeck, C., Skorochod, A., 2014. The Zotino Tall Tower Observatory (ZOTTO) quantifying large scale biogeochemical changes in Central Siberia. Nova Acta Leopoldina NF 117, Nr. 399, 51–64.

Hogg, E.H., Hurdle, P.A., 1997. Sap flow in trembling aspen: implications for stomatal responses to vapor pressure deficit. Tree Physiol. 17, 501–509.

Hollinger, D.Y., Kelliher, F.M., Byers, J.N., Hunt, J.E., Mcseveny, T.M., Weir, P.L., 1994. Carbon dioxide exchange between an undisturbed old-growth temperate forest and the atmosphere. Ecology 75, 134–150. http://dx.doi.org/10.2307/1939390.

Horst, T.W., 1997. A simple formula for attenuation of eddy fluxes measured with first-order-response scalar sensors. Boundary-Layer Meteorol. 82, 219–233. http://dx.doi.org/10.1023/A:1000229130034.

Jarvis, P.G., Massheder, J.M., Hale, S.E., Moncrieff, J.B., Rayment, M., Scott, S.L., 1997. Seasonal variation of carbon dioxide, water vapor, and energy exchanges of a boreal black spruce forest. J. Geophys. Res. 102, 28953–28966. http://dx.doi.org/10.1029/97JD01176.

Jing, X., Huang, J., Wang, G., Higuchi, K., Bi, J., Sun, Y., Yu, H., Wang, T., 2010. The effects of clouds and aerosols on net ecosystem CO_2 exchange over semi-arid Loess Plateau of Northwest China. Atmos. Chem. Phys. 10, 8205–8218. http://dx.doi.org/10.5194/acp-10-8205-2010.

Kanniah, K.D., Beringer, J., Tapper, N.J., Long, C.N., 2010. Aerosols and their influence on radiation partitioning and savanna productivity in northern Australia. Theor. Appl. Climatol. 100, 423–438. http://dx.doi.org/10.1007/s00704-009-0192-z.

Kanniah, K., Beringer, J., North, P., Hutley, L., 2012. Control of atmospheric particles on diffuse radiation and terrestrial plant productivity: A review. Prog. Phys. Geogr. 36, 209–237. http://dx.doi.org/10.1177/0309133311434244.

Kaufman, Y.J., Koren, I., 2006. Smoke and pollution aerosol effect on cloud cover. Science 313, 655. http://dx.doi.org/10.1126/science.1126232.

Kelliher, F.M., Hollinger, D.Y., Schulze, E.D., Vygodskaya, N.N., Byers, J.N., Hunt, J.E., McSeveny, T.M., Milukova, I., Sogatchev, A., Varlargin, A., Ziegler, W., Arneth, A., Bauer, G., 1997. Evaporation from an eastern Siberian larch forest. Agric. For. Meteorol. 85, 135–147. http://dx.doi.org/10.1016/S0168-1 923(96)02424-0.

Kelliher, F.M., Lloyd, J., Arneth, A., Lühker, B., Byers, J.N., Mcseveny, T.M., Milukova, I., Grigoriev, S., Panfyorov, M., Sogatchev, A., Varlargin, A., Ziegler, W., Bauer, G., Wong, S.-C., Schulze, E.-D., 1999. Carbon dioxide efflux density from the floor of a central Siberian pine forest. Agric. For. Meteorol. 94, 217–232. http://dx.doi.org/10.1016/S0168-1923(99)00014-3.

Kirschbaum, M.U.F., Eamus, D., Gifford, R.M., Roxburgh, S.H., Sands, P.J., 2001. Definitions of some ecological terms commonly used in carbon accounting. In: Kirschbaum, M.U.F., Mueller, R. (Eds.), Proceedings of the Net Ecosystem Exchange CRC Workshop. CRC for Greenhouse Accounting, Canberra. pp. 2–5.

Knohl, A., Baldocchi, D.D., 2008. Effects of diffuse radiation on canopy gas exchange processes in a forest ecosystem. J. Geophys. Res. G: Biogeosci. 113, G02023. http://dx.doi.org/10.1029/2007JG000663.

Kolle, O., Rebmann, C., 2007. EddySoft – Documentation of a Software Package to Acquire and Process Eddy Covariance Data, Technical Reports 10 Max-Planck-Institut für Biogeochemie, Jena, Germany pp 88.

Konovalov, I.B., Berezin, E.V., Ciais, P., Broquet, G., Beekmann, M., Hadji-Lazaro, J., Clerbaux, C., Andreae, M.O., Kaiser, J.W., Schulze, E.D., 2014. Constraining CO_2 emissions from open biomass burning by satellite observations of co-emitted species: a method and its application to wildfires in Siberia. Atmos. Chem. Phys. 14, 10383–10410. http://dx.doi.org/10.5194/acp-14-10383-2014.

Koren, I., Kaufman, Y.J., Remer, L.A., Martins, J.V., 2004. Measurement of the effect of Amazon smoke on inhibition of cloud formation. Science 303, 1342–1345. http://dx.doi.org/10.1126/science.1089424.

Kozlova, E.A., Manning, A.C., Kisilyakhov, Y., Seifert, T., Heimann, M., 2008. Seasonal, synoptic, and diurnal-scale variability of biogeochemical trace gases and O_2 from a 300-m tall tower in central Siberia. Glob. Biogeochem. Cycles 2, GB4020. http://dx.doi.org/10.1029/2008GB003209.

Larcher, W., 2003. Physiological Plant Ecology: Ecophysiology and Stress Physiology of Funtional Groups. Springer Verlag, Berlin. http://dx.doi.org/10.1007/978-3-662-05214-3.

Letts, M.G., Lafleur, P.M., Roulet, N.T., 2005. On the relationship between cloudiness and net ecosystem carbon dioxide exchange in a peatland ecosystem. Écoscience 12, 53–59. http://dx.doi.org/10.2980/i1195-6860-12-1-53.1.

Levy, R.C., Remer, L.A., Kleidman, R.G., Mattoo, S., Ichoku, C., Kahn, R., Eck, T.F., 2010. Global evaluation of the Collection 5 MODIS dark-target aerosol products over land. Atmos. Chem. Phys. 10, 10399–10420. http://dx.doi.org/10.5194/acp-10-10399-2010.

Liu, H., Peters, G., Foken, T., 2001. New equations for sonic temperature variance and buoyancy heat flux with an omnidirectional sonic anemometer. Boundary-Layer Meteorol. 100, 459–468. http://dx.doi.org/10.1023/A:1019207031397.

Lloyd, J., Shibistova, O., Zolotoukhine, D., Kolle, O., Arneth, A., Wirth, C., Styles, J.M., Tchebakova, N.M., Schulze, E.-D., 2002. Seasonal and annual variations in the photosynthetic productivity and carbon balance of a central Siberian pine forest. Tellus 54B, 590–610. http://dx.doi.org/10.1034/j.1600-0889.2002.01487.x.

Los, S.O., Collatz, G.J., Sellers, P.J., Malmström, C.M., Pollack, N.H., DeFries, R.S., Bounoua, L., Parris, M.T., Tucker, C.J., Dazlich, D.A., 2000. A global 9-yr biophysical land surface dataset from NOAA AVHRR data. J. Hydrometeorol. 1, 183–199. http://www.jstor.org/stable/24909292.

Lovett, G.M., Cole, J.J., Pace, M.L., 2006. Is net ecosystem production equal to ecosystem carbon accumulation? Ecosystems 9, 152–155. http://dx.doi.org/10.1007/s10021-005-0036-3.

Mammarella, I., Launiainen, S., Gronholm, T., Keronen, P., Pumpanen, J., Rannik, Ü., Vesala, T., 2009. Relative humidity effect on the high-frequency attenuation of water vapor flux measured by a closed-path eddy covariance system. J. Atmos. Ocean. Technol. 26, 1856–1866. http://dx.doi.org/10.1175/2009JTECHA1179.1.

Mammarella, I., Peltola, O., Nordbo, A., Järvi, L., Rannik, Ü., 2016. Quantifying the uncertainty of eddy covariance fluxes due to the use of different software packages and combinations of processing steps in two contrasting ecosystems. Atmos. Meas. Tech. 9, 4915–4933. http://dx.doi.org/10.5194/amt-9-4915-2016.

Matsui, T., Beltrán-Przekurat, A., Niyogi, D., Pielke Sr., R.A., Coughenou, M., 2008. Aerosol light scattering effect on terrestrial plant productivity and energy fluxes over the eastern United States. J. Geophys. Res. 113, D14S14. http://dx.doi.org/10.1029/2007JD009658.

Mercado, L.M., Bellouin, N., Sitch, S., Boucher, O., Huntingford, C., Wild, M., Cox, P.M., 2009. Impact of changes in diffuse radiation on the global land carbon sink. Nature 458, 1014–1017. http://dx.doi.org/10.1038/nature07949.

Migliavacca, M., Meroni, M., Manca, G., Matteucci, G., Montagnani, L., Grassi, G., Zenone, T., Teobaldelli, M., Goded, I., Colombo, R., Seufert, G., 2009. Seasonal and interannual patterns of carbon and water fluxes of a poplar plantation under peculiar eco-climatic conditions. Agric. For. Meteorol. 149, 1460–1476. http://dx.doi.org/10.1016/j.agrformet.2009.04.003.

Min, Q., 2005. Impacts of aerosols and clouds on forest-atmosphere carbon exchange. J. Geophys. Res. D Atmos. 110, D06203. http://dx.doi.org/10.1029/2004JD004858.

Misson, L., Lunden, M., McKay, M., Goldstein, A.H., 2005. Atmospheric aerosol light scattering and surface wetness influence the diurnal pattern of net ecosystem exchange in a semi-arid ponderosa pine plantation. Agric. For. Meteorol. 129, 69–83. http://dx.doi.org/10.1016/j.agrformet.2004.11.008.

Moffat, A.M., Beckstein, C., Churkina, G., Mund, M., Heimann, M., 2010. Characterization of ecosystem responses to climatic controls using artificial neural networks. Glob. Change Biol. 16, 2737–2749. http://dx.doi.org/10.1111/j.1365-2486.2010.02171.x.

Moffat, A.M., 2012. A new methodology to interpret high resolution measurements of net carbon fluxes between terrestrial ecosystems and the atmosphere. PhD Thesis. Friedrich-Schiller-Universität, Jena.

Moon, K.J., Kim, J., Cho, H.K., Lee, J., Hong, S.Y., Jeong, M.J., 2009. Effect of aerosol optical depth on diffuse photosynthetically active solar irradiance. Asia-Pac. J. Atmos. Sci. 45 (3), 307–317.

Musavi, T., Migliavacca, M., van de Weg, M.J., Kattge, J., Wohlfahrt, G., van Bodegom, P.M., Reichstein, M., Bahn, M., Carrara, A., Domingues, T.F., Gavazzi, M., Gianelle, D., Gimeno, C., Granier, A., Gruening, C., Havránková, K., Herbst, M., Hrynkiw, C., Kalhori, A., Kaminski, T., Klumpp, K., Kolari, P., Longdoz, B., Minerbi, S., Montagnani, L., Moors, E., Oechel, W.C., Reich, P.B., Rohatyn, S., Rossi, A., Rotenberg, E., Varlagin, A., Wilkinson, M., Wirth, C., Mahecha, M.D., 2016. Potential and limitations of inferring ecosystem photosynthetic capacity from leaf functional traits. Ecol. Evol. 6, 7352–7366. http://dx.doi.org/10.1002/ece3.2479.

Niyogi, D., Chang, H.-I., Saxena, V.K., Holt, T., Alapaty, K., Booker, F., Chen, F., Davis, K.J., Holben, B., Matsui, T., Meyers, T., Oechel, W.C., Pielke S, R.A., Wells, R., Wilson, K., Xue, Y., 2004. Direct observations of the effects of aerosol loading on net ecosystem CO_2 exchanges over different landscapes. Geophys. Res. Lett. 31, L20506. http://dx.doi.org/10.1029/2004GL020915.

Oliphant, A.J., Dragoni, D., Deng, B., Grimmond, C.S.B., Schmid, H.P., Scott, S.L., 2011. The role of sky conditions on gross primary production in a mixed deciduous forest. Agric. For. Meteorol. 151, 781–791. http://dx.doi.org/10.1016/j.agrformet.2011.01.005.

Oliveira, P.H.F., Artaxo, P., Pires, C., De Lucca, S., Procópio, A., Holben, B., Schafer, J., Cardoso, L.F., Wofsy, S.C., Rocha, H.R., 2007. The effects of biomass burning aerosols and clouds on the CO_2 flux in Amazonia. Tellus 59B, 338–349. http://dx.doi.org/10.1111/j.1600-0889.2007.00270.x.

Papale, D., Reichstein, M., Aubinet, M., Canfora, E., Bernhofer, C., Kutsch, W., Longdoz, B., Rambal, S., Valentini, R., Vesala, T., Yakir, D., 2006. Towards a standardized processing of net ecosystem exchange measured with eddy covariance technique: algorithms and uncertainty estimation. Biogeosciences 3, 571–583. http://dx.doi.org/10.5194/bg-3-571-2006.

Ponomarev, E., Kharuk, V., Ranson, K., 2016. Wildfires dynamics in Siberian larch forests. Forests 7, 125. http://dx.doi.org/10.3390/f7060125.

Ponomarev, E.I., 2013. Radiative power of wildfires in Siberia on the basis of TERRA/MODIS imagery processing. Folia For. Pol. Ser. A 55, 102–110. http://dx.doi.org/10.2478/ffp-2013-00011.

R Core Team 2016, 2016. R: A Language and Environment for Statistical Computing. R Foundation for Statistical Computing, Vienna, Austria URL. https://www.R-project.org/.

Rannik, Ü., Vesala, T., 1999. Autoregressive filtering versus linear detrending in estimation of fluxes by the eddy covariance method. Boundary-Layer Meteorol. 91, 259–280. http://dx.doi.org/10.1023/A:1001840416858.

Rap, A., Spracklen, D.V., Mercado, L., Reddington, C.L., Haywood, J.M., Ellis, R.J., Phillips, O.L., Artaxo, P., Bonal, D., Coupe, N.R., Butt, N., 2015. Fires increase Amazon forest productivity through increases in diffuse radiation. Geophys. Res. Lett. 42, 1–9. http://dx.doi.org/10.1002/2015GL063719.

Reichstein, M., Bahn, M., Mahecha, M.D., Kattge, J., Baldocchi, D.D., 2014. Linking plant and ecosystem functional biogeography. Proc. Natl. Acad. Sci. U. S. A. 111, 13697–13702. http://dx.doi.org/10.1073/pnas.1216065111.

Remer, L., Kleidman, R.G., Levy, R.C., Kaufman, Y.J., Tanré, D., Mattoo, S., Martins, J.V., Ichoku, C., Koren, I., Yu, H., et al., 2008. Global aerosol climatology from the MODIS

satellite sensors. J. Geophys. Res. 113. http://dx.doi.org/10.1029/2007JD009661.
Rocha, A.V., Su, H.-B., Vogel, C.S., Schmid, H.P., Curtis, P.S., 2004. Photosynthetic and water use efficiency responses to diffuse radiation by an aspen-dominated northern hardwood forest. For. Sci. 50, 793–801.
Roderick, M.L., Farquhar, G.D., Berry, S.L., Noble, I.R., 2001. On the direct effect of clouds and atmospheric particles on the productivity and structure of vegetation. Oecologia 129, 21–30. http://dx.doi.org/10.1007/s004420100760.
Schafer, J.S., Eck, T.F., Holben, B.N., Artaxo, P., Yamasoe, M.A., Procopio, A.S., 2002a. Observed reductions of total solar irradiance by biomass-burning aerosols in the Brazilian Amazon and Zambian Savanna. Geophys. Res. Lett. 29, 1823. http://dx.doi.org/10.1029/2001GL014309.
Schafer, J.S., Holben, B.N., Eck, T.F., Yamasoe, M.A., Artaxo, P., 2002b. Atmospheric effects on insolation in the Brazilian Amazon: observed modification of solar radiation by clouds and smoke and derived single scattering albedo of fire aerosols. J. Geophys. Res. D Atmos. 107, 8074. http://dx.doi.org/10.1029/2001JD000428.
Schulze, E.-D., Vygodskaya, N.N., Tchebakova, N.M., Czimczik, C.I., Kozlov, D.N., Lloyd, J., Mollicone, D., Parfenova, E., Sidorov, K.N., Varlagin, A.V., Wirth, C., 2002. The eurosiberian transect: an introduction to the experimental region. Tellus 54B, 421–428. http://dx.doi.org/10.1034/j.1600-0889.2002.01342.x.
Shibistova, O., Lloyd, J., Zrazhevskaya, G., Arneth, A., Kolle, O., Knohl, A., Astrakhantchva, N., Shijneva, I., Schmerler, J., 2002. Annual ecosystem respiration budget for a *Pinus sylvestris* stand in central Siberia. Tellus 54B, 568–589. http://dx.doi.org/10.3402/tellusb.v54i5.16688.
Steiner, A.L., Mermelstein, D., Cheng, S.J., Twine, T.E., Oliphant, A., 2013. Observed impact of atmospheric aerosols on the surface energy budget. Earth Interact. 17, 1–22. http://dx.doi.org/10.1175/2013EI000523.1.
Still, C.J., Riley, W.J., Biraud, S.C., Noone, D.C., Buenning, N.H., Randerson, J.T., Torn, M.S., Welker, J., White, J.W.C., Vachon, R., Farquhar, G.D., Berry, J.A., 2009. Influence of clouds and diffuse radiation on ecosystem-atmosphere CO_2 and $CO^{18}O$ exchanges. J. Geophys. Res. G: Biogeosci. 114, G01018. http://dx.doi.org/10.1029/2007JG000675.
Strada, S., Unger, N., 2016. Potential sensitivity of photosynthesis and isoprene emission to direct radiative effects of atmospheric aerosol pollution. Atmos. Chem. Phys. 16, 4213–4234. http://dx.doi.org/10.5194/acp-16-4213-2016.
Strada, S., Unger, N., Yue, X., 2015. Observed aerosol-induced radiative effect on plant productivity in the eastern United States. Atmos. Environ. 122, 463–476. http://dx.doi.org/10.1016/j.atmosenv.2015.09.051.
Tautenhahn, S., Lichstein, J.W., Jung, M., Kattge, J., Bohlman, S.A., Heilmeier, H., Prokushkin, A., Kahl, A., Wirth, C., 2016. Dispersal limitation drives successional pathways in Central Siberian forests under current and intensified fire regimes. Glob. Change Biol. 22, 2178–2197. http://dx.doi.org/10.1111/gcb.13181.
Tchebakova, N.M., Parfenova, E., Soja, A.J., 2009. The effects of climate, permafrost and fire on vegetation change in Siberia in a changing climate. Environ. Res. Lett. 4, 045013. http://dx.doi.org/10.1088/1748-9326/4/4/045013.
Tchebakova, N.M., Vygodskaya, N.N., Arneth, A., Marchesini, L.B., Kolle, O., Kurbatova, Y.A., Parfenova, E.I., Valentini, R., Vaganov, E.A., Schulze, E.-D., 2015. Energy and mass exchange and the productivity of main Siberian ecosystems (from Eddy covariance measurements). 1. heat balance structure over the vegetation season. Biol. Bull. 42, 570–578. http://dx.doi.org/10.1134/S1062359015660012.
Tishkov, A., 2002. Boreal forests. In: Shahgedanova, M. (Ed.), The physical geography of Northern Eurasia. Oxford University Press, Oxford, pp. 216–233.
Urban, O., Janouš, D., Acosta, M., Czerný, R., Marková, I., Navrátil, M., Pavelka, M., Pokorný, R., Šprtová, M., Zhang, R., Špunda, V., Grace, J., Marek, M.V., 2007. Ecophysiological controls over the net ecosystem exchange of mountain spruce stand. Comparison of the response in direct vs. diffuse solar radiation. Glob. Change Biol. 13, 157–168. http://dx.doi.org/10.1111/j.1365-2486.2006.01265.x.
Valendik, E.N., Verkhovets, S.V., Ponomarev, E.I., Ryzhkova, V.A., Kisilyakhov, Y.K., 2014. Large wildfires in taiga subzones of central Siberia. J. Sib. Fed. Univ. Biol. 1, 43–56.
Vasileva, A.V., Moiseenko, K.B., Mayer, J.C., Jürgens, N., Panov, A., Heimann, M., Andreae, M.O., 2011. Assessment of the regional atmospheric impact of wildfire emissions based on CO observations at the ZOTTO tall tower station in central Siberia. J. Geophys. Res. D Atmos. 116, D07301. http://dx.doi.org/10.1029/2010JD014571.
Vickers, D., Mahrt, L., 1997. Quality control and flux sampling problems for tower and aircraft data. J. Atmos. Oceanic Technol. 14, 512–526. http://dx.doi.org/10.1175/1520-0426(1997)014<0512:QCAFSP>2.0.CO;2.
Williams, M., Rastetter, E.B., Van der Pol, L., Shaver, G.R., 2014. Arctic canopy photosynthetic efficiency enhanced under diffuse light, linked to a reduction in the fraction of the canopy in deep shade. New Phytol. 202, 1267–1276. http://dx.doi.org/10.1111/nph.12750.
Winderlich, J., Chen, H., Gerbig, C., Seifert, T., Kolle, O., Lavrič, J.V., Kaiser, C., Höfer, A., Heimann, M., 2010. Continuous low-maintenance $CO_2/CH_4/H_2O$ measurements at the Zotino Tall Tower Observatory (ZOTTO) in Central Siberia. Atmos. Meas. Tech. 3, 1113–1128. http://dx.doi.org/10.5194/amt-3-1113-2010.
Winderlich, J., Gerbig, C., Kolle, O., Heimann, M., 2014. Inferences from CO_2 and CH_4 concentration profiles at the Zotino Tall Tower Observatory (ZOTTO) on regional summertime ecosystem fluxes. Biogeosciences 11, 2055–2068. http://dx.doi.org/10.5194/bg-11-2055-2014.
Wirth, A.C., Schulze, E.-D., Schulze, W., von Stünzner-Karbe, D., Ziegler, W., Miljukolva, I.M., Sogatchev, A., Varlagin, A.B., Panvyorov, M., Grigoriev, S., Kusnetzova, W., Siry, M., Hardes, G., Zimmermann, R., Vygodskaya, N.N., 1999. Above-ground biomass and structure of pristine Siberian Scots Pine forests as controlled by competition and fire. Oecologia 121, 66–80. http://dx.doi.org/10.1007/s004420050908.
Wohlfahrt, G., Hammerle, A., Haslwanter, A., Bahn, M., Tappeiner, U., Cernusca, A., 2008. Disentangling leaf area and environmental effects on the response of the net ecosystem CO_2 exchange to diffuse radiation. Geophys. Res. Lett. 35, L16805. http://dx.doi.org/10.1029/2008GL035090.
Yamasoe, M., Randow, C., Von Manzi, A., Schafer, J., Eck, T., Holben, B., Yamasoe, M., Randow, C., Von Manzi, A., Schafer, J., Eck, T., 2006. Effect of smoke on the transmissivity of photosynthetically active radiation inside the canopy. Atmos. Chem. Phys. 6, 1645–1656. http://dx.doi.org/10.5194/acp-6-1645-2006.
Zhuravleva, T.B., Kabanov, D.M., Nasrtdinov, I.M., Russkova, T.V., Sakerin, S.M., Smirnov, A., Holben, B.N., 2017. Radiative characteristics of aerosol during extreme fire event over Siberia in summer 2012. Atmos. Meas. Tech. Discuss. 10, 179–198. http://dx.doi.org/10.5194/amt-2016-244.